

# Surface Activity, Micelle Formation, and Growth of *n*-Octyl- $\beta$ -D-Thioglucopyranoside in Aqueous Solutions at Different Temperatures

J. A. Molina-Bolívar, J. Aguiar, J. M. Peula-García, and C. Carnero Ruiz\*

Departamento de Física Aplicada II, Escuela Universitaria Politécnica, Universidad de Málaga, Campus de El Ejido, s/n, 29013 - Málaga, Spain

Received: May 6, 2004; In Final Form: June 25, 2004

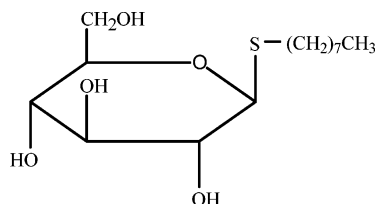
Micellization, surface activity, and structures of the aggregates of the nonionic surfactant *n*-octyl- $\beta$ -D-thioglucopyranoside in aqueous solutions through a temperature range have been investigated. By using surface tension measurements, information was obtained on both changes in the critical micelle concentration and adsorption behavior in the air–liquid interface with the temperature. These data were used to obtain the thermodynamic properties of micellization along with the corresponding adsorption parameters in the air–liquid interface. The results obtained indicated that the surfactant headgroup has a more pronounced hydrophilic character than that of the common polyoxyethylenic nonionic surfactants. Size and structure of the micelles formed at different temperatures were investigated by light scattering measurements. The light scattering data, including static and dynamic experiments, account for micelle growth and hydration. The analysis of the experimental results was focused on the phase transition from sphere to rodlike structures. To corroborate this point, additional measurements of density and intramolecular excimer formation of 1,2-dipyrenylpropane versus the surfactant concentration were performed. Satisfactory agreement of the results, showing a significant micellar growth starting from a certain surfactant concentration, was observed by means of the different techniques used.

## Introduction

Surfactants are extensively used in numerous applications in the biomembrane field. Most of them involve solubilization and purification of biopolymers from their natural matrixes by selective solubilization.<sup>1</sup> For these applications, surfactant with properties such as high solubilizing power, high critical micelle concentration (cmc), no denaturation of proteins, high solubility in water, and stability are preferred.<sup>2</sup> Alkylpolyglucosides (APGs) are nonionic surfactants, characterized by having a hydroxyl sugar group as a hydrophilic moiety, which are attracting increasing interest because they enjoy many of the properties mentioned above. Besides, these surfactants are biodegradable and considered dermatologically safe and, therefore, are materials very interesting in applications related to cosmetic preparations, cleaning products, or food technology.<sup>3</sup> On the other hand, they show a solution behavior substantially different from the ethoxylated nonionic surfactants. Namely, APGs have both stronger lipophobicity and hydrophilicity, and their temperature dependence of the solution properties is much less pronounced, not showing the clouding phenomenon.<sup>4,5</sup> This almost temperature insensitivity of their physicochemical properties arises from the strength of the hydrogen bonds between the hydroxy groups of the sugar group and water and, therefore, the headgroup dehydration when the temperature increase is much less significant.<sup>6</sup>

Among the APG surfactants, octyl- $\beta$ -D-glucopyranoside (OG) has been probably the most widely investigated, and a number of studies on its physicochemical properties have been recently carried out.<sup>1,7–13</sup> Octyl- $\beta$ -D-thioglucopyranoside (OTG) is a related nonionic surfactant that differs from OG only in how

## CHART 1: Molecular Structure of OTG



the hydrophilic group is linked by a thioether to the hydrophobic chain (Chart 1), which seems to be responsible for its different solution behavior in comparison with OG. For instance, the cmc for OTG has been determined to be about 9 mM, a low value compared to 23–25 mM for OG, suggesting a more hydrophobic character for the former.<sup>2</sup> In addition, OTG shows a superior stability to that of OG.<sup>2</sup> Contrary to OG, OTG has been scarcely used in membrane research,<sup>14</sup> and, therefore, their solution properties have been much less studied. However, recent investigations<sup>2,14,15</sup> have revealed the advantages of OTG against OG in the membrane protein field. For a deeper understanding of the interaction of OTG with biomolecules and for the use of this surfactant on a more rational basis, a detailed study on their solution behavior and structural properties is required. In this context, we have decided to carry out an investigation on the physicochemical properties of OTG, including micellization, adsorption in the air–liquid interface, and structures of the aggregates as a function of temperature. With this purpose, we have used techniques such as surface tension and static and dynamic light scattering (DLS). The outline of this paper is as follows: First, by using surface tension measurements we have obtained the cmc values and the adsorption behavior in the air–liquid interface at different temperatures. From these data, we have determined the thermodynamic properties of micellization

\* Corresponding author. E-mail: ccarnero@uma.es.

and the corresponding parameters of adsorption. Second, we have performed a combined study of static and DLS measurement in a temperature range, which has allowed us to obtain information on important structural aspects of the micellar aggregates. In addition, with the aim of examining possible micellar phase transitions, we present complementary results based on density measurements and on the formation of intramolecular excimers of 1,2-dipyrrenylpropane solubilized in the micellar phase.

## Experimental Section

**Materials.** The surfactant OTG and the fluorescence probe pyrene were purchased from Sigma Co., whereas 1,3-dipyrrenylpropane (P3P) was obtained from Molecular Probes. All these compounds were certified to be of high purity and, therefore, were used as received. Stock solutions of the surfactant were prepared in double distilled water, and those of the fluorescence probes in absolute ethanol. All these solutions were stored at 4 °C. Work solutions were used immediately after preparation.

**Surface Tension Measurements.** These measurements were performed in a Sigma 701 (KSV) tensiometer by the Wilhelmy plate method after appropriate calibration. The temperature was maintained constant by circulating thermostated water through a jacketed vessel containing the solution. The surface tension measurements were started with a concentrated solution of surfactant, and successive diluted solutions were obtained by adding doubly distilled water to the vessel. The equilibrium state was checked by taking a number of measurements after 15-min intervals until no significant change occurred. At least 10 measurements of surface tension for each concentration were carried out. The standard deviation of these measurements was always lower of  $\pm 0.08$  mN/m.

**Light Scattering Measurements.** Particles in solution scatter light as a result of the difference in the refractive index of the particles and the solvent. In this work, light scattering measurements were carried out at 25, 35, and 45 °C with a Malvern System 4700 equipped with a 75-mW Ar ion laser emitting vertically polarized light at 488 nm as a light source. The sample temperature was stabilized by a thermostatic bath within  $\pm 0.1$  °C. The sample cells were soaked in nitric acid and rinsed with distilled water and finally with freshly distilled acetone before use. Surfactant solutions were filtered once through a 0.1- $\mu$ m Millipore filter directly into the cell and sealed until use. This operation removed any dust particles present.

DLS measurements were carried out to determine the translational diffusion coefficients and associated apparent hydrodynamic radius of the micelles. By using the data treatment described in a previous paper<sup>16,17</sup> we have obtained the so-called apparent diffusion coefficient ( $D_c$ ) by

$$D_c = \Gamma/q^2 \quad (1)$$

where  $q$  is the scattering wave vector. For small macromolecules, the diffusion coefficient is a function only of the concentration of the solution. This is due to the interparticle interaction hindering the free motion in the solvent. To obtain the free diffusion coefficient  $D_0$ , one extrapolates the measured values to zero concentration. From that result one can evaluate the apparent hydrodynamic radius of the micelles,  $R_H$ , from the Stokes–Einstein relation

$$R_H = \frac{k_B T}{6\pi\eta_0 D_0} \quad (2)$$

where  $k_B T$  is the thermal energy factor and  $\eta_0$  is the solvent viscosity.  $R_H$  coincides with the real hydrodynamic radius of the micelles only when they are spherical. In the case of the rodlike micelle, we obtain from this equation an average equivalent sphere hydrodynamic radius (apparent hydrodynamic radius). The diffusion coefficient was measured at least three times for each sample. The average error in these experiments was estimated to be 4%.

Static light scattering data provide information on the average molecular weight of the micelles,  $M_w$ , and the second virial coefficient  $B_2$ . For an uncharged macromolecule, the second virial coefficient depends on the volume of the molecule and on the nature of the solvent–solute interaction.<sup>18</sup> According to the Rayleigh–Gans–Debye theory, the scattered intensity of light from a dilute solution of weakly interacting particles with small dimensions compared with the wavelength of the incident light (i.e., diameter  $< \lambda/20$ ) may be approximated by

$$\frac{K(c - \text{cmc})}{\Delta R_\theta} = \frac{1}{M_w P(q)} + 2B_2(c - \text{cmc}) \quad (3)$$

where  $c$  is the total surfactant concentration,  $M_w$  is the micelle molecular weight,  $P(q)$  is the particle form factor, and  $K$  is an optical constant given by

$$K = \frac{4\pi^2 n_0^2 (dn/dc)^2}{N_A \lambda_0^4} \quad (4)$$

where  $n_0$  is the solvent refractive index,  $dn/dc$  is the refractive index increment of the micellar solution, and  $\lambda_0$  is the wavelength of incident light. The refractive index values of the solvent and micellar solutions were measured at 25, 35, and 45 °C using a digital Abbe refractometer (WYA-1S). The refractive index increment was determined by fitting  $n$  as a linear function of the surfactant concentration.

The particle form factor at small scattering angles can be approximated by

$$\frac{1}{P(\theta)} = 1 + \frac{16\pi^2 n_0^2}{3\lambda^2} R_G^2 \sin^2 \frac{\theta}{2} \quad (5)$$

irrespectively of micelle shape, where  $R_G$  is the radius of gyration of the micelles. If the micelles are polydisperse,  $M_w$  is their weight-average molecular weight and  $R_G$  is their some-higher-order-average radius of gyration. If the scattering angle is extrapolated to zero or if there is no angular dependence of light scattering (i.e., when the particle size is much smaller than the wavelength of light), the value of  $P(q)$  is unity.

The parameter  $\Delta R_\theta$  is the so-called excess scattering ratio of the micelles which is obtained from the difference in the Rayleigh ratio between the micellar solution and the solvent solution in the absence of micelles,  $\Delta R_\theta = R_\theta - R_\theta^0$ . On the other hand, the Rayleigh ratio of the sample solution is determined using toluene as a standard according to the relationship

$$R_\theta = \frac{I_\theta}{I_{\text{tol}}} R_{\text{tol}} \quad (6)$$

where  $I_\theta$  and  $I_{\text{tol}}$  are the scattered intensity of the sample solution and the toluene, respectively, and  $R_{\text{tol}}$  is the Rayleigh ratio of toluene. This value was assumed to be  $31.6 \times 10^{-4} \text{ m}^{-1}$  at 488 nm. The intensity of scattered light was measured at least four

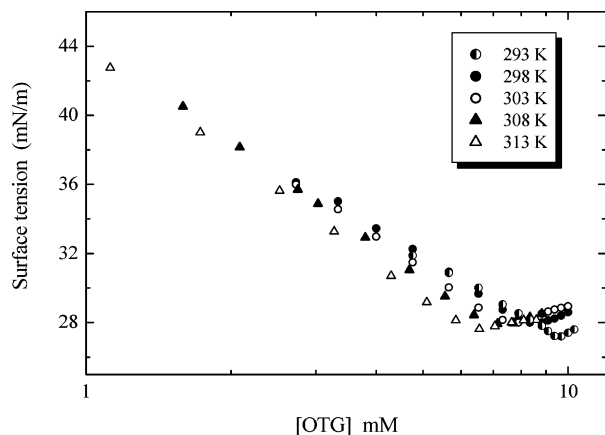


**Figure 1.** Surface tension isotherms of OTG at different temperatures.

times for each sample. The average error in these repeated measurements was approximately 2%.

**Fluorescence Measurements.** A Spex FluoroMax-2 spectrofluorometer was used for all fluorescence measurements. This instrument is equipped with a thermostated cell housing that allowed temperature control to  $\pm 0.1$  °C. To determine the cmc of OTG at 25 °C, the fluorescence emission spectra of pyrene (1  $\mu$ M) in OTG solutions of different concentrations were recorded employing the “S” mode with band-passes for excitation and emission monochromators of 1.05 nm and an excitation wavelength of 335 nm. From these spectra, the intensities  $I_1$  and  $I_3$  were measured at the wavelength corresponding to the first and the third vibronic band located near 372 and 384 nm. The ratio  $I_1/I_3$  is the so-called pyrene 1:3 ratio. Similarly, the emission spectra of P3P (1.8  $\mu$ M) in micellar OTG solutions were obtained between 350 and 550 nm by using the same recording mode and band-passes and an excitation wavelength of 346 nm. The intensities of the emission of the monomer ( $I_M$ ) was recorded at the wavelength corresponding to the first vibronic peak of the monomer, located near 378 nm, and that of the excimer ( $I_E$ ) at around 490 nm. The solutions for excimer forming studies were prepared by adding the appropriate volumes of a concentrated P3P ethanolic solution to aqueous surfactant solutions. These solutions were then sonicated during 1 h and kept for equilibration on a bath at 25 °C for at least 12 h.

**Density Measurements.** Density measurements were performed with an Anton-Paar DMA 58 density meter. This apparatus determines the density value by placing the sample in a U-shaped tube and measuring its period of oscillation. The instrument has an accuracy of  $\pm 1 \times 10^{-5}$  g/cm<sup>3</sup>, and it was calibrated with air and water at 25 °C. The temperature was controlled within  $\pm 0.01$  °C.

## Results and Discussion

**cmc and Thermodynamics of Micellization.** The surface tension of OTG micellar solutions was measured as a function of the surfactant concentration at various temperatures. Figure 1 shows the plots of surface tension versus the logarithm of the surfactant concentration at different temperatures. In these plots a minimum is observed, which is usually attributed to the presence of impurities. However, it must be noted that there are several cases in the literature<sup>19,20</sup> in which other APG surfactants show a similar behavior. In any way, to corroborate that this minimum does not affect the cmc determination, we have obtained the cmc of OTG at 25 °C by using a different experimental technique, as described below. The plots in Figure

**TABLE 1: cmc Values and Thermodynamic Parameters of Micellization for OTG at Different Temperatures**

<i>T</i> (K)	cmc (mM)	$-\Delta G_{\text{mic}}^0$ (kJ/mol)	$\Delta H_{\text{mic}}^0$ (kJ/mol)	$T\Delta S_{\text{mic}}^0$ (kJ/mol)
293	9.3	21.18	14.35	35.53
298	8.5 (8.7) <sup>a</sup>	21.76	14.84	36.60
303	7.5	22.44	15.34	37.78
308	6.9	23.02	15.85	38.87
313	6.2	23.66	16.37	40.03

<sup>a</sup> cmc value as obtained by the pyrene 1:3 ratio method.

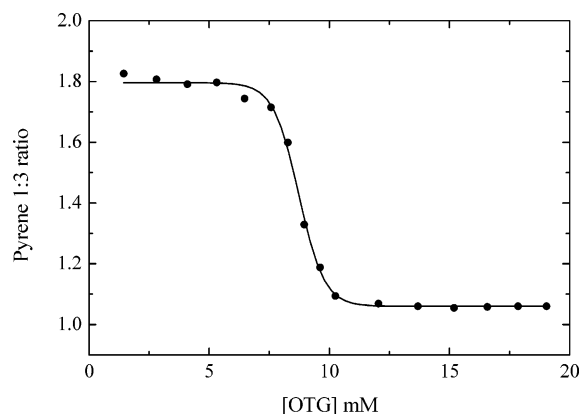


**Figure 2.** Plot of pyrene 1:3 ratio versus concentration of OTG at 25 °C.

1 show a sharp breakpoint which corresponds to the cmc value at each temperature, as listed in Table 1. The cmc at 25 °C was determined, by triplicate experiments, to be  $8.5 \pm 0.2$  mM, a lower value than that obtained by Zana and co-workers<sup>8</sup> by the pyrene 1:3 ratio method (9.2 mM). Therefore, we decided to carry out the cmc determination at this temperature by the same method. The result of this experiment is presented in Figure 2. As recently discussed,<sup>21</sup> the cmc can be obtained from the pyrene 1:3 ratio plots by using two different approaches: (i) from the interception of the rapidly varying part and the nearly horizontal part at high surfactant concentration or (ii) from the inflection point of the corresponding plot. The value of 9.2 mM determined by the aforementioned authors was obtained by the first approach; however, we have obtained a value of 8.7 mM, in very good agreement to that obtained by surface tension measurements, by using the second approach.

Data in Table 1 show that the cmc of OTG decreases as the system temperature increases in the temperature range studied. This trend is a consequence of the reduction in hydrophobicity of the surfactant molecules, which is due to a smaller probability of hydrogen bond formation at higher temperatures. In other words, the increase in temperature produces the decrease in hydration of the hydrophilic headgroup, which favors the micellization process. Therefore, the micellization process occurs at lower concentrations as the temperature increases.

We have used the temperature dependence of the cmc of OTG to obtain the corresponding thermodynamic parameters of micellization. According to the mass action or the phase separation model, the standard free energy of micelle formation per mole of monomer,  $\Delta G_{\text{mic}}^0$ , in the case of a nonionic surfactant, is given by<sup>22</sup>

$$\Delta G_{\text{mic}}^0 = RT \ln x_{\text{cmc}} \quad (7)$$

where  $x_{\text{cmc}}$  is the mole fraction of surfactant at the cmc.

By applying the Gibbs–Helmholtz equation to eq 7, the enthalpy of micellization can be obtained by



$$\Delta H_{\text{mic}}^0 = -RT^2 \left( \frac{\partial \ln x_{\text{cmc}}}{\partial T} \right)_P \quad (8)$$

In this way, the enthalpy of micellization can be evaluated from the slope of the plot of  $\ln x_{\text{cmc}}$  versus temperature. This plot (not shown) presents a linear relationship ( $r = 0.998$ ) between both variables in the temperature range examined.

The entropy contribution to the micellization process can be estimated from the calculated enthalpy and free energy values as

$$T\Delta S_{\text{mic}}^0 = \Delta H_{\text{mic}}^0 - \Delta G_{\text{mic}}^0 \quad (9)$$

The thermodynamic parameters of micellization that we have obtained by applying the above procedure are also reported in Table 1. The free energy of micellization is negative and becomes more negative as the temperature increases, indicating that the formation of micelles becomes more spontaneous at higher temperatures. The data of the change of the enthalpy of micellization,  $\Delta H_{\text{mic}}^0$ , that we have obtained indicate that the micellization process is endothermic ( $\Delta H_{\text{mic}}^0 > 0$ ); however, this magnitude shows a weak dependence with temperature. Positive values of  $\Delta H_{\text{mic}}^0$ , such as those observed in our system, are usually attributed to the release of structural water from the hydration layers around the hydrophobic parts of the surfactant molecule.<sup>23</sup> These hydrophobic interactions become significantly smaller with the partial disruption of the structure of the water as the temperature is increased. The entropic contribution of the micelle formation,  $T\Delta S_{\text{mic}}^0$ , presents positive values that are larger than  $\Delta H_{\text{mic}}^0$ , showing the importance of hydrophobic interactions in the micellization process of OTG. The so-called enthalpy–entropy compensation<sup>24</sup> has been observed in many processes, including micellization of surfactants, which is reflected by a linear relationship between the enthalpy change and the entropy change, its slope being the so-called compensation temperature. We have observed a good linearity ( $r = 0.999$ ) in the compensation plot for our system, and the value found for the compensation temperature is around 302 K. This value lies near of the range 270–300 K, which has been used as a diagnostic test for the participation of water in the protein reaction.<sup>25</sup> It must be noted here that the compensation temperature that we have determined is smaller than those found for different homologous series of ethoxylated nonionic surfactants (322 K for C<sub>8</sub>E<sub>6</sub> and 328 K for OPE<sub>6</sub>), but very similar to that of certain homologous series of ionic surfactants, including alkyl sulfates (304 K) and alkyltrimethylammonium bromides (308 K).<sup>24</sup> This fact suggests that the hydrophilic group of OTG behaves more similarly to the mentioned ionic surfactants than to the nonionic ones. In fact, the existence of a small but significant charge in APG micelles has been previously established.<sup>26</sup>

**Thermodynamics of Adsorption.** An effective measure of the adsorption of surfactant in the air–liquid interface is usually obtained by the surface excess concentration,  $\Gamma_{\text{max}}$ , which can be determined, for dilute solutions, by the Gibbs equation<sup>27</sup>

$$\Gamma_{\text{max}} = - \frac{1}{RT} \left[ \frac{\partial \gamma}{\partial \ln c} \right]_{T,P} \quad (10)$$

where  $R$  and  $T$  have their usual meaning,  $\gamma$  is the corrected surface tension, and  $c$  is the concentration of surfactant. From the surface excess concentration, it is possible to calculate the

**TABLE 2: Surface Excess Concentration ( $\Gamma_{\text{max}}$ ), Minimum Area per Molecule ( $A_{\text{min}}$ ), Surface Pressure at the cmc ( $\Pi_{\text{cmc}}$ ), and Gibbs Energy of Adsorption ( $\Delta G_{\text{ads}}^0$ ) for OTG at Different Temperatures**

$T$ (K)	$\Gamma_{\text{max}} \times 10^3$ (mmol/m <sup>2</sup> )	$A_{\text{min}}$ (Å <sup>2</sup> /molecule)	$\Pi_{\text{cmc}}$ (mN/m)	$-\Delta G_{\text{ads}}^0$ (kJ/mol)
293	2.84	58.56	44.99	37.05
298	3.06	54.33	43.69	36.05
303	3.24	51.30	42.86	35.68
308	3.41	48.70	42.21	35.40
313	3.44	48.27	41.51	35.73

minimum area per surfactant molecule,  $A_{\text{min}}$ , at the air–solvent interface, by the equation

$$A_{\text{min}} = \frac{1}{N_A \Gamma_{\text{max}}} \quad (11)$$

where  $N_A$  is Avogadro's number. The effectiveness of a surface-active molecule is measured by the surface pressure at the cmc,  $\Pi_{\text{cmc}}$ , which can be obtained from the relationship

$$\Pi_{\text{cmc}} = \gamma_0 - \gamma_{\text{cmc}} \quad (12)$$

Here,  $\gamma_0$  and  $\gamma_{\text{cmc}}$  are the surface tension of pure solvent and of the micellar solution at the cmc, respectively.

The standard free energy of adsorption,  $\Delta G_{\text{ads}}^0$ , was determined using the equation

$$\Delta G_{\text{ads}}^0 = \Delta G_{\text{mic}}^0 - \frac{\Pi_{\text{cmc}}}{\Gamma_{\text{max}}} \quad (13)$$

where the standard state for the surface phase is defined as a hypothetical surface covered with a monolayer of surfactant at its closest packing but at a surface pressure equal to zero.<sup>27</sup> The adsorption parameters obtained for our systems are listed in Table 2. From the data in Table 2, it can be seen that the surface excess concentration,  $\Gamma_{\text{max}}$ , increases slightly with temperature. This behavior is due to the fact that hydration of the hydrophilic group decreases as the temperature increases and, therefore, increases the tendency to locate at the air–liquid interface. The moderate increase in the effectiveness of adsorption with temperature is due to increased thermal motion. As expected,  $A_{\text{min}}$  presents an inverse trend with temperature. The  $A_{\text{min}}$  value is 58.56 Å<sup>2</sup> or less, suggesting that the hydrophobic chains of the surfactant adsorbed at the air–liquid interface are not in close-packed arrangement normal to the interface at saturation adsorption.<sup>27</sup> A priori, an increase in the adsorption of the surfactant should produce a decrease in the surface tension and, therefore, an increase in the surface pressure ( $\Pi_{\text{cmc}}$ ). However, in our case, the reduction rate in  $\gamma_0$  is greater than in  $\gamma_{\text{cmc}}$ , resulting in a decrease of  $\Pi_{\text{cmc}}$ , as shown in Table 2. We think that this fact can be interpreted in the sense that temperature has a greater effect on the water structure than on the dehydration of the hydrophilic groups of the surfactant.

From data in Table 2 it can be seen that  $\Delta G_{\text{ads}}^0$  values are negative and become less negative as the temperature increases, indicating that the adsorption of the surfactant in the air–liquid interface occurs spontaneously and becomes more spontaneous at higher temperatures. This can be attributed to the fact that dehydration of the hydrophilic groups, which is required for the adsorption process, is facilitated as temperature increases. In addition, it is observed that  $\Delta G_{\text{ads}}^0$  values are more negative than their corresponding  $\Delta G_{\text{mic}}^0$  values, indicating that when a OTG micelle is formed, work has to be done to transfer the

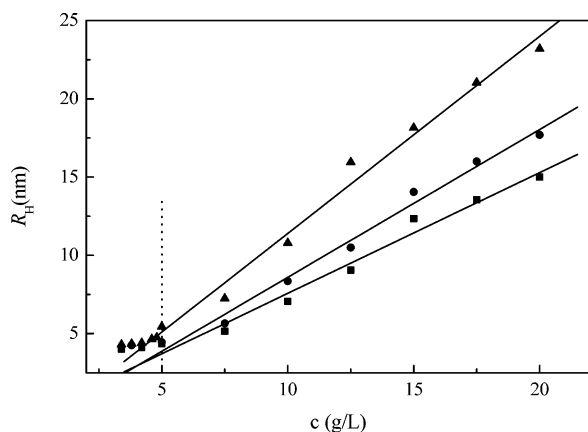


**Figure 3.** Apparent hydrodynamic radius,  $R_H$ , of OTG micelles as a function of surfactant concentration at different temperatures: (▲) 25, (●) 35, and (■) 45 °C.

**TABLE 3: Structural Parameter of OTG Micelles as a Function of Temperature, As Obtained in the Concentration Range from 3 to 5 g/L**

$T$ (°C)	$M_w$ (Da)	$N_{agg}$	$B_2 \times 10^8$ (mol m <sup>3</sup> g <sup>-2</sup> )	$R_H^0$ (nm)	$R_{EFF}$ (nm)
25	35 040	114	-1.46	3.5	12.1
35	36 200	117	-1.28	3.5	11.8
45	35 900	116	-0.78	3.5	9.9

surfactant molecules in the monomeric form at the surface to the micellar stage through the aqueous medium.<sup>28,29</sup>

**Size and Structure of the Aggregates.** In Figure 3 the apparent hydrodynamic radius of OTG micelles versus the surfactant concentration at various temperatures is plotted. As can be seen, the results showed a well-pronounced transition in the micelle size at a certain surfactant concentration. At surfactant concentrations lower than this transition surfactant concentration (around 5 g/L), the micelle size presents a weak dependence on surfactant concentration. In this region of low surfactant concentration, micelles are small and it is plausible to suppose that they have a spherical shape. After the break point in the curve a strong concentration dependence of the micelle size which rapidly increases is observed. The data indicate a significant micellar growth with the corresponding change in the micelle shape from sphere to rodlike. The monotonic increase of  $R_H$  with OTG concentration found in the present work is similar to those reported previously for ionic surfactant micelles in electrolyte solutions by different authors.<sup>30,31</sup> Micellar solutions present some peculiarity with respect to typical colloid solutions, particularly because micelles may change size and shape by changing either the surfactant concentration or the temperature. Although the present study of light scattering does not provide us with any explicit information about the micelle shape, it is accepted in the literature that spherical surfactant micelles undergo a transition to larger rodlike aggregates with the surfactant concentration because large micelles cannot be accommodated in the globular micelle.<sup>32</sup> Figure 3 shows that the micellar growth is more significant at low temperature, suggesting that the formation of rodlike micelles is enhanced by the decreasing of the temperature.<sup>33</sup> The actual diffusion coefficients,  $D_0$ , were obtained by extrapolation of the data at infinite dilution ( $c = 0$ ). From  $D_0$  the hydrodynamic radius  $R_H^0$  was determined by eq 2. The values obtained are listed in Table 3, where it is noteworthy that the hydrodynamic radius of OTG micelles is independent of temperature. This fact is in line with analogous results obtained for octyl- $\beta$ -glucoside micellar solutions.<sup>34</sup>

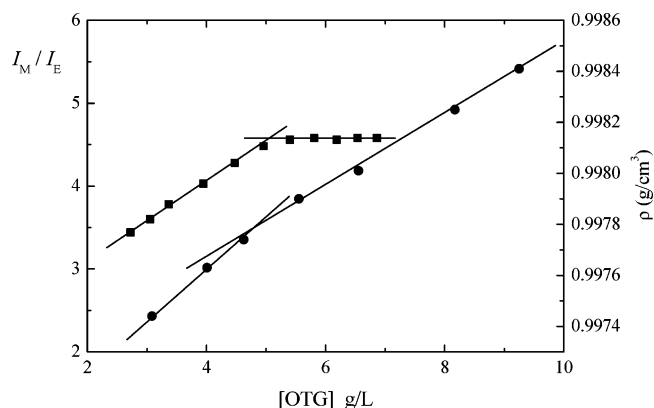


**Figure 4.** Effect of the surfactant concentration on the intramolecular excimer forming of P3P (■) and the density of micellar solutions of OTG (●) at 25 °C.

Additional experimental evidence supporting the existence of a sphere-to-rod transition was obtained from two different techniques at 25 °C, density and intramolecular excimer forming of P3P measurements as a function of surfactant concentration. These two techniques were chosen because they give different perspectives of the system. The former reports information on a macroscopic property whereas the latter does it on a microscopic one such as the micellar microviscosity. In Figure 4 we present the results obtained by the above experiments. It is well-known that the degree of intramolecular excimer formation of P3P depends on the local viscosity of the probe imposed by its microenvironment. In fact, the monomer-to-excimer intensity ratio,  $I_M/I_E$ , gives a qualitative index of the microviscosity as sensed by the probe.<sup>35</sup> It has been shown that the microviscosity increases when the micelles grow in size and become elongated with increasing surfactant concentration.<sup>36–38</sup> When this phase transition is accomplished, the microviscosity levels off. This is just the behavior observed for our system in Figure 4. By the comparison of the behavior of the apparent micelle radius and the micellar microviscosity index, the observed break in the  $I_M/I_E$  is closely related to the increase of the micelle size. In the cited figure it can be seen that the density plot shows a break point at a similar surfactant concentration. This result suggests that this break in density could be attributed to a transition in micellar shape from sphere to rodlike. The surfactant concentration corresponding to the phase transition is the so-called secondary cmc. Beyond this secondary cmc, the primary spherical micelles are in equilibrium with the secondary large rodlike micelles.<sup>39–41</sup>

The critical micellization concentration can also be determined by measuring the average intensity of the scattered light as a function of the surfactant concentration. The appearance of micelles leads to a break point in the concentration dependence, after which the intensity of the scattered light increases with the concentration. Figure 5 shows the scattered light intensity at  $\theta = 90^\circ$  as a function of surfactant concentration at three temperatures. The amount of light scattered is nearly constant at very low surfactant concentrations, but it suddenly increases beyond a surfactant concentration of 3 g/L. This can be ascribed to the formation of micelles. A strong increase in scattering intensity at all temperatures is observed. This type of behavior has been observed in some cationic surfactant systems where it was attributed to unidirectional growth of micelles.<sup>42–44</sup> On the other hand, each plot consists of two sections. In the range 3–5 g/L, the linearity of the curves is satisfactory. However, for concentrations higher than 5 g/L the scattered light intensity increases steadily with a concave curvature downward, sug-

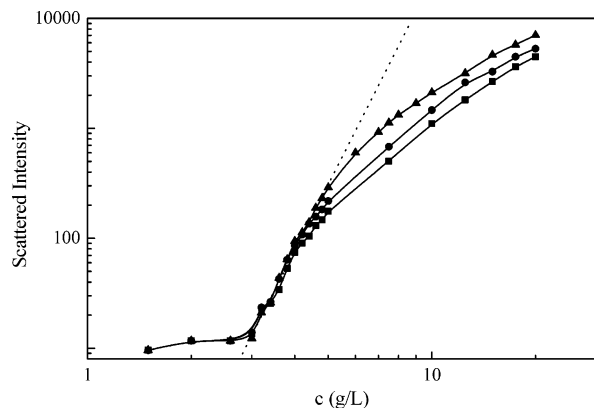


**Figure 5.** Change of light scattering intensity with OTG concentration at different temperatures: (▲) 25, (●) 35, and (■) 45 °C.

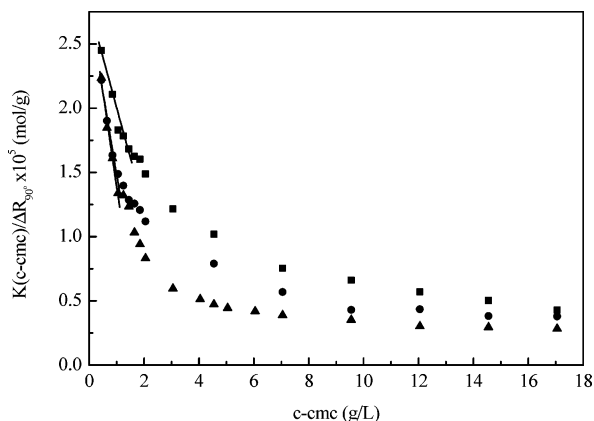


**Figure 6.** Debye plots for OTG solutions at various temperatures: (▲) 25, (●) 35, and (■) 45 °C. Light scattering is in the 90° direction.

gesting that the micelles could associate into large micelles with increasing surfactant concentration. For all temperatures studied, the transition of micelle shape occurs in OTG solutions of concentrations well above the cmc. Probably the OTG solution with high surfactant concentration contains, at least, two kinds of micelles, that is, the small spherical micelles formed at the cmc and the large micelles, and the latter fraction increases with increasing the OTG concentration.

The intensity of scattered light depends on both the molecular weight of the micelles and the micellar interactions. The analysis of static light scattering data was based on the eq 3. The results are represented as plots of  $K(c - \text{cmc})/\Delta R_{90}$  against  $c - \text{cmc}$  (the so-called Debye plot) in Figure 6. As can be seen, the results show a strongly initial decrease with increasing surfactant concentration and then level off at high concentrations. An apparent linearity is observed in the range of low surfactant concentration (where spherical micelles are present). We may infer that the micelle growth is promoted by the increase in micelle concentration above a certain value. From this point, the micelles associate into larger micelles (rodlike shape) and the results deviate downward from a straight line.<sup>45</sup> Linear regression analysis of the initial part of the data in this figure [assuming that  $P(\theta) = 1$ ] was used to estimate the micellar molecular weight of OTG micelles in the respective temperature, and, hence, we obtained the corresponding mean micellar aggregation number values. On the other hand, the second virial coefficient can be obtained from the slope of linear regression. The calculated values are listed in Table 3. The aggregation number is seen to be nearly invariant in the temperature range studied. Our value of the aggregation number of OTG in water is in agreement with that obtained by Zana et al. by using time-

resolved fluorescence experiments.<sup>8</sup> It must be pointed out that the value that we have found is greater than those reported for other surfactants with an octyl chain.<sup>7,37</sup> Similar results have been previously found by Aoudia and Zana.<sup>46</sup> These authors suggest that probably the sugar surfactant micelles are anisotropic and the micellar shape is not spherical even near the cmc.

Another interesting result is the negative slope of the lines in Figure 6, indicating an attractive interaction between OTG micelles and solvent. The  $B_2$  values are less negative with increasing the temperature of micellization, suggesting a decrease in attractive interactions. The second virial coefficient for macromolecules of any architecture can be expressed in terms of a sphere volume (the so-called effective volume,  $V_{\text{EFF}}$ ) that is equivalent to a hard, homogeneous sphere. The value of the effective volume accounts for the micelle interactions, and its value for particles interacting as hard spheres is equal to the actual micelle volume ( $V_s$ ). In contrast,  $V_{\text{EFF}}$  could be substantially different from  $V_s$  if long-range interactions are present.  $V_{\text{EFF}}$  can be expressed through the second virial coefficient:<sup>47</sup>

$$V_{\text{EFF}} = \frac{1}{4} \frac{B_2 M_w^2}{N_A} \quad (14)$$

Further, from  $V_{\text{EFF}}$  we estimated the effective radius of micelles ( $R_{\text{EFF}}$ ) as a function of temperature. The calculated values are presented in Table 3. We find that  $R_{\text{EFF}}$  as determined by static light scattering is higher than the actual hydrodynamic radius  $R_H^0$ , which is due to the long-ranged attraction between the OTG micelles and solvent. Some authors suggest that the negative virial coefficient could be a consequence of the increase in micellar size with surfactant concentration.<sup>7,48</sup>

Kameyama and Takagi have observed that the second virial coefficient of OG micelles, determined by light scattering, increases with the temperature, changing the sign from negative to positive at 40 °C.<sup>7</sup> Comparing the  $B_2$  values determined by the aforementioned authors ( $-2.3 \times 10^{-7} \text{ mol m}^3 \text{ g}^{-2}$  at 22 °C) with those obtained in the present work, we could suggest that OTG micelles have a less hydrated structure than those formed by OG. In fact, Zana et al. have justified the fact that the cmc of OTG is less than half that of OG, indicating that the  $-S-$  group is much more hydrophobic than the  $-O-$  group.<sup>8</sup> On the other hand, the  $B_2$  values obtained by Imae<sup>49</sup> for heptaoxyethylene alkyl ethers ( $C_nE_7$ ) through static light scattering experiments ( $-0.08 \times 10^{-11} \text{ mol m}^3 \text{ g}^{-2}$  to  $-2.14 \times 10^{-11} \text{ mol m}^3 \text{ g}^{-2}$ ) are much smaller than those reported in the present study. This may suggest that the interfaces of the sugar surfactant micelles (OTG) are probably more hydrated than those of ethylene oxide-based nonionic surfactants.

One of the characteristic features of nonionic surfactants is that they often exhibit a critical phenomenon of demixing. When the isotropic micellar phase is heated, a critical temperature is reached at which solutions become suddenly turbid (cloud point). At this temperature, a liquid–liquid phase separation occurs. It is assumed that the phase separation is due to the reduction of the intermicellar repulsions, as a result of the dehydration of the oxyethylene groups as the temperature is increased. Contrary to  $C_iE_j$  surfactants (ethoxylated nonionic surfactants), the sugar surfactants do not show the clouding phenomena when the temperature is raised.<sup>4,5</sup> In fact, we have checked this point in our laboratory for the case of OTG. On the contrary, light scattering studies previously carried out by us with Triton X-100, which presents the clouding phenomenon, revealed that the second virial coefficient for this nonionic surfactant is practically zero.<sup>17</sup> Therefore, the fact that OTG micelles present a high

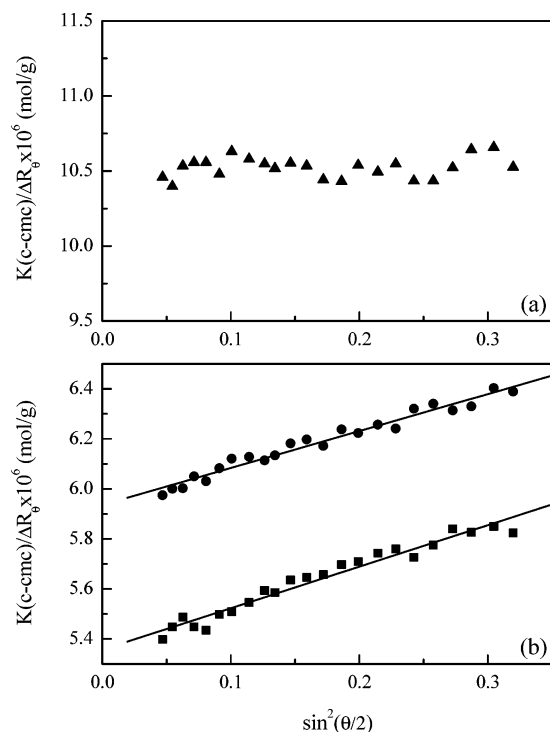


**Figure 7.** Angular dependence of light scattering from OTG solutions at 25 °C: (a) 5 and (b) 6 (●) and 7 g/L (■).

**TABLE 4: Characteristics of OTG Rodlike Micelles as a Function of Surfactant Concentration at 25 °C**

<i>c</i> (g/L)	<i>M<sub>w</sub></i> (Da)	<i>N<sub>agg</sub></i>	<i>R<sub>g</sub></i> (nm)	<i>R<sub>H</sub></i> (nm)	<i>ρ</i>
5	79624	258		4.9	
6	149142	484	24.5	5.9	4.1
7	170794	554	28	7.4	3.8

interaction with solvent, as previously mentioned, is consistent with the fact that these micelles are better hydrated than similar EO-based nonionic surfactants. Sugar-derived and EO-derived micelles differ in regard to their hydrogen-bonding interactions with water. There is extensive water content in the headgroups of both kinds of micelles, but the EO segments are hydrogen bond receptors and the sugar headgroups are both acceptors and donors.<sup>50</sup> This difference in the donor/acceptor balance allows the sugar headgroups, or their attached water molecules, to be much more effective than EO headgroups in hydrogen bonding.

To gain more insight into the growth of micelles from globular to rodlike structures, we have investigated the angular dependence of light scattering. Figure 7 shows the angular dependence of light scattering from OTG solutions at 5 g/L (Figure 7a) and 6 g/L and 7 g/L (Figure 7b) at 25 °C. As can be seen, the reciprocal angular envelope of light scattering linearly increases with increasing  $\sin^2(\theta/2)$  for 6 g/L and 7 g/L. This angular dependence of the light scattering accounts for the difference in the micellar size; the slope at low scattering angle is zero for the low surfactant concentration (5 g/L) but finite at high surfactant concentrations (6 g/L and 7 g/L). OTG is unlikely to form large rodlike micelles at a surfactant concentration lower than 5 g/L because no angular dependence was observed in light scattering, which corresponds to small spherical micelles. According to eqs 3 and 5, the intercept of the curve gives the reciprocal of the weight-average molecular weight,  $M_w$ , of the micelle at a given surfactant concentration assuming that  $B_2$  is negligible. From the value of the finite slope we can evaluate the radius of gyration (see Table 4). It is important to notice that to derive the exact value of these parameters, we have to take account of the contribution of the

second virial coefficient  $B_2$ . However, for micelles with a large molecular weight the contribution of the second virial coefficient can be neglected.<sup>51,52</sup> From data in Table 4 it is noteworthy that the mean aggregation number is too high to accommodate a spherical micelle. These elevated values of weight-average molecular weight cannot be assignable to a spherical micelle. At these surfactant concentrations rodlike micelles would be formed. Thus, the OTG surfactant forms spherical micelles at the cmc, but they associate into rodlike micelles as the micelle concentration is increased.

In micelles that grow significantly and exhibit angular dependence in static light scattering, additional information on micelle shape can be obtained by comparing the values of  $R_g$  and  $R_H$  (see Table 4). This relationship is usually expressed in terms of a dimensionless quantity  $\rho$  defined as<sup>53</sup>

$$\rho = R_g/R_H \quad (15)$$

For spherical micelles,  $\rho$  should be 0.775 whereas experimental data have suggested values of  $\rho$  ranging between 1.35 and 4 for rodlike aggregates.<sup>44,53–55</sup> The values obtained in the present work are 2.1 for 6 g/L and 1.90 for 7 g/L, suggesting that the micelles deviate from spherical geometry to rodlike. Scaling relationships can provide useful information on the conformation and flexibility of micelles. The scaling relationship between the molecular weight of micelles and the radius of gyration is sensitive to micelle shape:<sup>56</sup>

$$R_g \sim M_w^n \quad (16)$$

A double logarithmic plot of  $R_g$  versus the molecular weight of micelles presents an exponent  $n = 1.06$ . A value of 0.5 is characteristic of a random coil structure whereas rigid and thin rods are expected to give an exponent close to unity.<sup>56</sup>

## Conclusions

Surface tension and light scattering measurements were performed on OTG aqueous solutions in a temperature range. From the surface tension isotherms we have obtained information on both micellization and surface properties of the surfactant between 20 and 40 °C. The results indicated that the micellization process is favored by a temperature increase, showing an enthalpy–entropy compensation typical process in aqueous medium. The adsorption data in the air–liquid interface showed that the adsorption of the surfactant occurs spontaneously and becomes more spontaneous at higher temperatures. Using DLS we have determined the apparent hydrodynamic radius of the micelles. The data indicated a significant micellar growth when the surfactant concentration is higher than 5 g/L. The micelles are spherical at low surfactant concentration, but they become rodlike at high surfactant concentration. The rodlike structures decrease in size as the temperature increases at a given surfactant concentration. The mean aggregation number and the second osmotic virial coefficient of the spherical micelles were determined from static light scattering measurements. The results obtained indicated that the mean aggregation number is practically unaffected with the temperature, whereas the virial coefficient increases. To prove the change in the micelle shape, complementary measurements of density and intramolecular excimer forming of P3P as a function of the surfactant concentration were carried out. These results are in accordance with the formation of larger structures from a certain surfactant concentration.



**Acknowledgment.** This work has been financially supported by the Spanish Science and Technology Ministry (Project No. MAT2001-1743). The authors wish to thank Prof. R. Hidalgo-Álvarez, Group of Fluid Physics and Biocolloids of the University of Granada, for providing light scattering research facilities.

## References and Notes

- (1) Bonincontro, A.; Briganti, G.; D'Aprano, A.; La Mesa, C.; Sesta, B. *Langmuir* **1996**, *12*, 3206.
- (2) Saito, S.; Tsuchiya, T. *Biochem. J.* **1984**, *222*, 829.
- (3) García, M. T.; Ribosa, I.; Campos, E.; Sanchez Leal, J. *Chemosphere* **1997**, *35*, 545.
- (4) Shinoda, K.; Carlsson, A.; Lindman, B. *Adv. Colloid Interface Sci.* **1996**, *64*, 253.
- (5) Söderman, O.; Johansson, I. *Curr. Opin. Colloid Interface Sci.* **2000**, *4*, 391.
- (6) Stubenrauch, C. *Curr. Opin. Colloid Interface Sci.* **2001**, *6*, 160.
- (7) Kameyama, K.; Takagi, T. *J. Colloid Interface Sci.* **1990**, *137*, 1.
- (8) Frindi, M.; Michels, B.; Zana, R. *J. Phys. Chem.* **1992**, *96*, 8137.
- (9) La Mesa, C.; Bonincontro, A.; Sesta, B. *Colloid Polym. Sci.* **1993**, *271*, 1165.
- (10) Antonelli, M. L.; Bonicelli, M. G.; Ceccaroni, G.; La Mesa, C.; Sesta, B. *Colloid Polym. Sci.* **1994**, *272*, 704.
- (11) Aoudia, M.; Zana, R. *J. Colloid Interface Sci.* **1998**, *206*, 158.
- (12) Pastor, O.; Junquera, E.; Aicart, E. *Langmuir* **1998**, *14*, 2950.
- (13) Whiddon, C. R.; Bunton, C. A.; Söderman, O. *J. Phys. Chem. B* **2003**, *107*, 1001.
- (14) Chami, M.; Pehau-Arnaudet, G.; Lambert, O.; Rank, J.-L.; Lévy, D.; Rigaud, J.-L. *J. Struct. Biol.* **2001**, *133*, 64.
- (15) Wenk, M. R.; Seelig, J. *Biophys. J.* **1997**, *73*, 2565.
- (16) Molina-Bolívar, J. A.; Aguiar, J.; Carnero Ruiz, C. *Mol. Phys.* **2001**, *99*, 1729.
- (17) Molina-Bolívar, J. A.; Aguiar, J.; Carnero Ruiz, C.; *J. Phys. Chem. B* **2002**, *106*, 870.
- (18) Tanford, C. *Physical Chemistry of Macromolecules*; John Wiley & Sons: New York, 1961.
- (19) von Rybinski, W.; Hill, K. *Angew. Chem., Int. Ed.* **1998**, *37*, 1328.
- (20) Sierra, M. L.; Svensson, M. *Langmuir* **1999**, *15*, 2301.
- (21) Aguiar, J.; Carpena, P.; Molina-Bolívar, J. A.; Carnero Ruiz, C. *J. Colloid Interface Sci.* **2003**, *258*, 116.
- (22) Myers, D. *Surfactant Science and Technology*; VCH: New York, 1992.
- (23) Krescheck, G. C. In *Water. A Comprehensive Treatise*; Franks, F., Ed.; Plenum: New York, 1975; Vol. 4, Chapter 2.
- (24) Chen, L.-J.; Lin, S.-Y.; Huang, C.-C. *J. Phys. Chem. B* **1998**, *102*, 4350.
- (25) Lumry, R.; Rajender, S. *Biopolymers* **1970**, *9*, 1125.
- (26) Balzer, D. *Langmuir* **1993**, *9*, 3375.
- (27) Rosen, M. J. *Surfactants and Interfacial Phenomena*; Wiley: New York, 1989.
- (28) Sulthana, S. B.; Bhat, S. G. T.; Rakshit, A. K. *Langmuir* **1997**, *13*, 4562.
- (29) Sulthana, S. B.; Rao, P. V. C.; Bhat, S. G. T.; Rakshit, A. K. *J. Phys. Chem. B* **1998**, *102*, 9653.
- (30) Schurtenberger, P.; Mazer, N.; Känzig, W. *J. Phys. Chem.* **1983**, *87*, 308.
- (31) Alargova, R.; Petkov, J.; Petsev, D.; Ivanov, I. B.; Broze, G.; Mehreteab, A. *Langmuir* **1995**, *11*, 1530.
- (32) Israelachvili, J. N. *Intermolecular and Surface Forces*; Academic Press: London, 1991.
- (33) Alargova, R. G.; Danov, K. D.; Petsov, J. T.; Kralchevsky, P. A.; Broze, G.; Mehreteab, A. *Langmuir* **1997**, *13*, 5544.
- (34) D'Aprano, A.; Giordano, R.; Jannelli, M. P.; Magazù, S.; Maisano, G.; Sesta, B. *J. Mol. Struct.* **1996**, *383*, 177.
- (35) Zana, R. *J. Phys. Chem. B* **1999**, *103*, 9117.
- (36) Miyagishi, S.; Suzuki, H.; Asakwa, T. *Langmuir* **1996**, *12*, 2900.
- (37) Zana, R. In M.; Lévy, H. Duportail, G. *Langmuir* **1997**, *13*, 5552.
- (38) Huang, J. B.; Zhao, G.-X. *Colloids Polym. Sci.* **1996**, *274*, 747.
- (39) Ozeki, S.; Ikeda, S. *Colloid Polym. Sci.* **1984**, *262*, 409.
- (40) Ozeki, S.; Ikeda, S. *J. Colloid Interface Sci.* **1982**, *87*, 424.
- (41) Missel, P. J.; Mazer, N. A.; Carey, M. C.; Benedek, G. B. *J. Phys. Chem.* **1989**, *96*, 8654.
- (42) Cates, M. E.; Candau, S. J. *J. Phys.: Condens. Matter* **1990**, *2*, 6869.
- (43) Herzog, B.; Huber, K.; Rennie, A. R. *J. Colloid Interface Sci.* **1994**, *164*, 370.
- (44) McDonald, J. A.; Rennie, A. R. *Langmuir* **1995**, *11*, 1493.
- (45) Hayashi, S.; Ikeda, S. *J. Phys. Chem.* **1980**, *84*, 744.
- (46) Aoudia, M.; Zana, R. *J. Colloid Interface Sci.* **1998**, *206*, 158.
- (47) Kralchevsky, P. A.; Danov, K. D.; Denkov, N. D. In *Handbook of Surface and Colloid Chemistry*; Birdi, K. S., Ed.; CRC Press: New York, 1999; Chapter 11.
- (48) Richtering, W. H.; Burchard, W.; Jahns, E.; Finkelmann, H. *J. Phys. Chem.* **1988**, *92*, 6032.
- (49) Imae, T. *J. Phys. Chem.* **1988**, *92*, 5721.
- (50) Whiddon, C. R.; Bunton, C. A.; Söderman, O. *J. Phys. Chem. B* **2003**, *107*, 1001.
- (51) Imae, T.; Kamiya, R.; Ikeda, S. *J. Colloid Interface Sci.* **1985**, *108*, 215.
- (52) Imae, T.; Ikeda, S. *J. Phys. Chem.* **1986**, *90*, 5216.
- (53) Schmidt, M. *Macromolecules* **1984**, *17*, 553.
- (54) Denking, P.; Burchard, W.; Kunz, M. *J. Phys. Chem.* **1989**, *93*, 1428.
- (55) Denking, P.; Kunz, W.; Burchard, W. *Colloid Polym. Sci.* **1990**, *268*, 513.
- (56) DeGennes, P. G. *Scaling Concepts in Polymer Physics*; Cornell University Press: Ithaca, NY, 1979.